Orientational Order-Dependent Thermal Expansion and Compressibility of ZrW_2O_8 and $ZrMo_2O_8$: Supplemental Material

Leighanne C. Gallington, Karena W. Chapman, Cody R. Morelock, Peter J. Chupas, and Angus P. Wilkinson

List of Figures

List of Tables

Sup. Fig. 1 Comparison of the MK3BRIM and MK2BRIM. Views from the beam stop blade side (upper left panel), beam entrance slits side (upper right panel), and top (lower panel). The top view shows the sample tube holes, side slot that allows easy flow of the pressure transmitting fluid past the BRIM, and a slot across the top that enables rotation of the BRIM in the pressure vessel bore during initial manual alignment.

The reported experiments made use of two slightly different Background Reducing Internal Mask (BRIM) designs, which are here referred to as MK2 and MK3. The key features of the MK2 design were previously described.[1] The MK3 design is slightly different and offers superior performance, principally a reduction in background from the titanium at "low" scattering angles and a decrease in the extent to which scattering from the sample at "low" angles is blocked by the beam stop. Photographs of the two different BRIMs from various angles are shown in Sup. Fig. 1.

In the MK2 design, the hole parallel to the BRIM axis for the sample was located on axis and had a diameter of ∼1.52 mm. The BRIM tungsten body had a diameter of 6.32 mm, which provides a snug sliding fit inside the pressure vessel body. The x-ray beam entrance slit was ∼0.3 mm wide and, at the bottom of this slit, there was a wide perpendicular slit that was used for initial x-ray alignment of the sample in the beam. The tungsten beam stop blade was 0.5 mm wide and 1 mm deep. The overall height of the BRIM body was 25.4 mm.

In the MK3 design, the hole parallel to the BRIM axis for the sample was located off axis so that it was further from the beam stop blade and closer to the x-ray entrance slit (hole axis off center by ∼0.508 mm). This reduces the extent to which the beam stop blade blocks scattering from the sample. The diameter of the hole for the sample was ∼1.016 mm, which further decreases the extent to which scattering from the sample is obscured by the beam stop blade but results in less overall signal. The BRIM body had a diameter of 6.22 mm, which provides a loose sliding fit in the grade 5 titanium pressure vessel bore. The loose fit relaxes the machining tolerances on the BRIM body and makes manufacture easier. Two coil springs were placed in slots around the circumference of the BRIM body so that the BRIM did not move in the bore of the pressure vessel after it was initially pushed into place. The x-ray beam entrance slit was ∼0.2 mm wide and, at the bottom of this slit, there was a large diameter round hole that was used for initial x-ray alignment of the sample in the beam. A hole was used rather than inverted "T", as it is easier to machine. The rhenium beam stop blade was 0.5 mm wide and 1 mm deep. The overall height of the BRIM body was 19.05 mm.

$T_{nominal}$	$T_{sample,MK2BRIM}$	$T_{sample,MK3BRIM}$
298K	298K	298K
343K	343K	343K
358K	357K	–
373K	371K	–
388K	386K	386K
403K	401K	–
418K	416K	–
433K	430K	430K
478K	473K	473K
523K	516K	516K

Sup. Table 1 Results of temperature calibration of the MK2BRIM and MK3BRIM. A thermocouple was epoxied inside a capillary, which was subsequently inserted into one of the BRIMs. The high pressure environment was assembled as previously described.[1] Temperatures in the capillary (T_{sample}) were recorded ∼30 min after the heating block reached the programmed temperature ($T_{nominal}$). The maximum discrepancy between the nominal and measured sample temperatures was ∼7K.

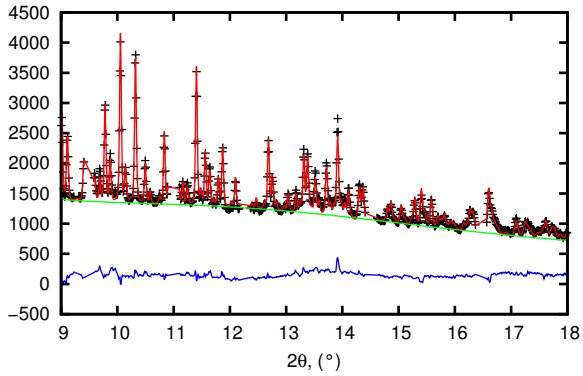

Sup. Fig. 2 Rietveld fit ($P2_13$ high temperature model) to ZrW_2O_8 data collected at 430K and 276 MPa in the MK2BRIM. Data points are indicated by black crosses, fit by red line, background by green line, and difference curve by blue line. A few narrow 2θ intervals were excluded due to the presence of substantial parasitic titanium scattering from the pressure cell.

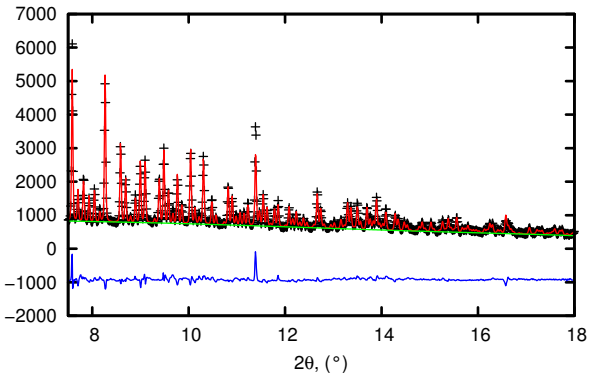

Sup. Fig. 3 Rietveld fit ($P2_13$ high temperature model) to ZrW_2O_8 data collected at 386K and 103 MPa in the MK3BRIM. Data points are indicated by black crosses, fit by red line, background by green line, and difference curve by blue line. Use of the MK3BRIM allowed for Rietveld fitting down to a lower 2θ limit and fewer excluded regions as compared with the MK2BRIM due to its greater efficacy in reducing parasitic titanium scattering from the pressure cell. The two noticeable peaks in the difference curve are believed to be due to parasitic titanium scattering from the pressure cell; however, this contamination was much lower in this dataset than the MK2BRIM dataset in the same 2θ regions, so these regions were not excluded from Rietveld analysis.

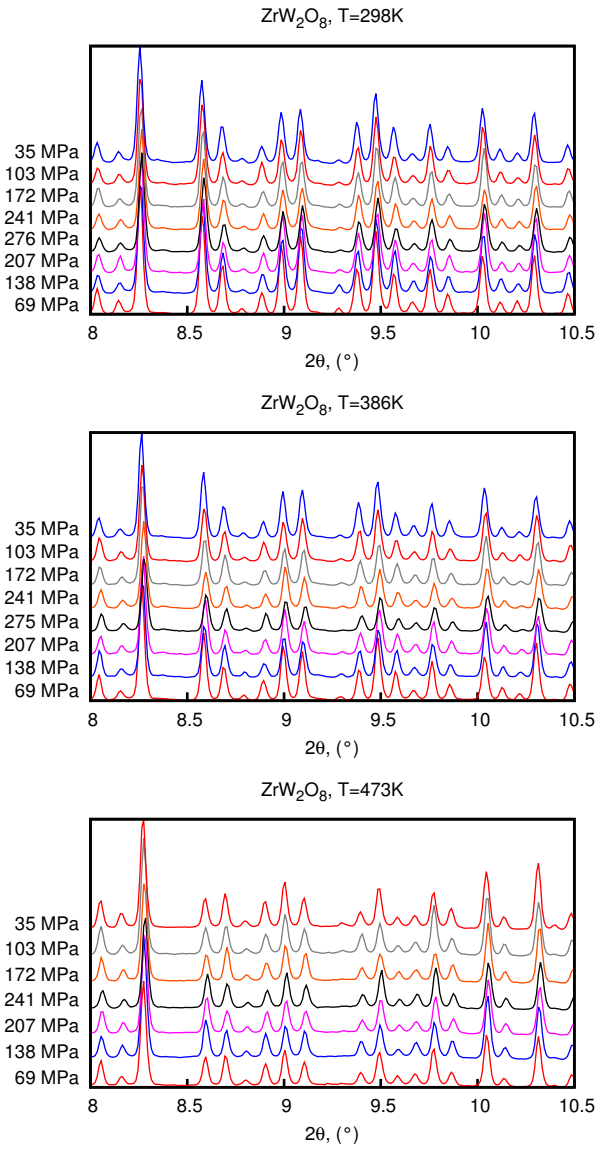

Sup. Fig. 4 Integrated diffraction data from ZrW_2O_8 experiment conducted in the MK3BRIM. Data are arranged in order of collection from bottom to top in each plot. Noticeable structural changes upon compression can be observed at 386K, particularly at the set of peaks just above 8.5°.

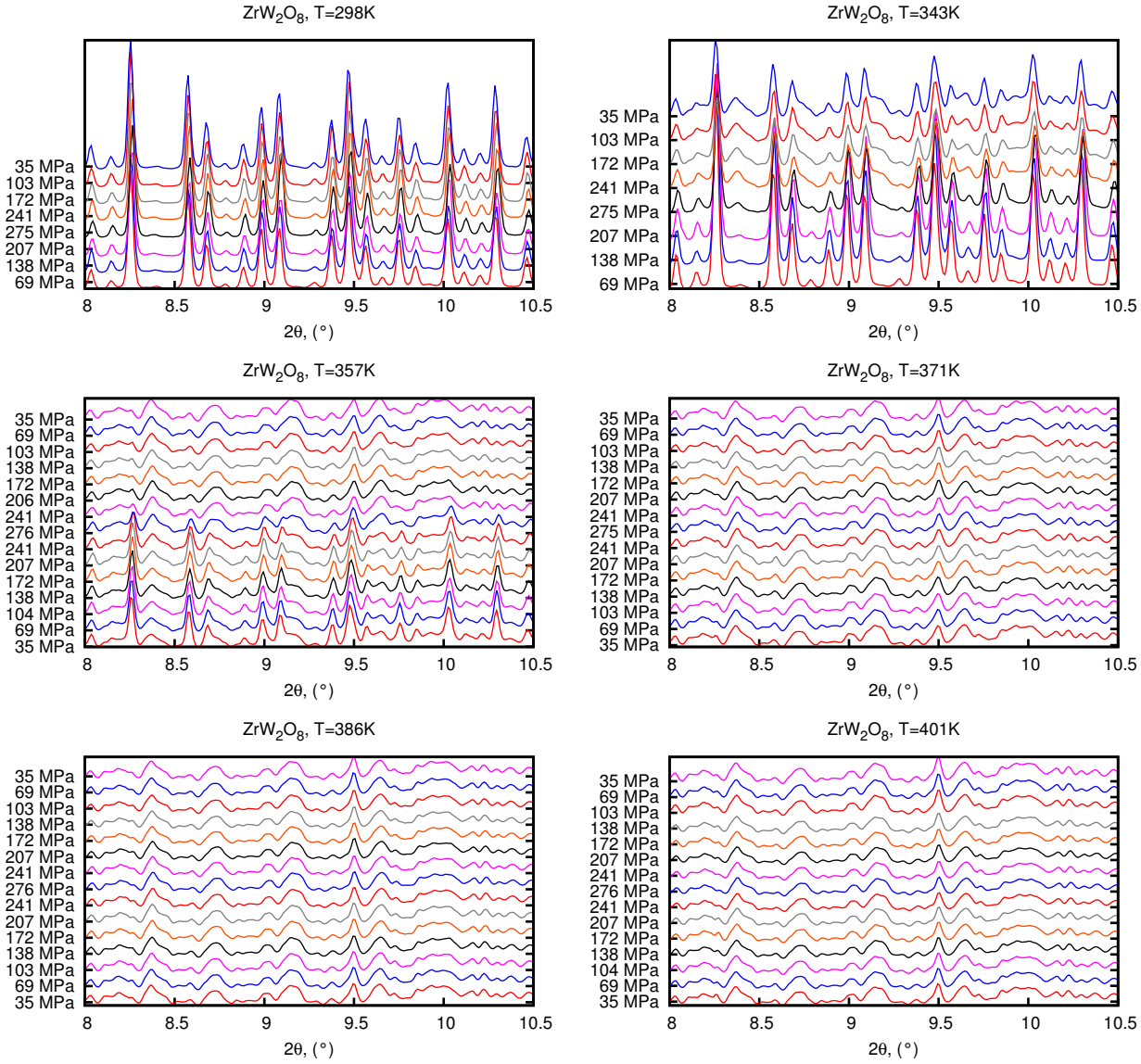

Sup. Fig. 5 Integrated diffraction data from ZrW_2O_8 experiment conducted in the MK2BRIM, 298-401K. Data are arranged in order of collection from bottom to top in each plot. The $\alpha \rightarrow \gamma$ transition induced by compression can be visually tracked at 343K and 357K.

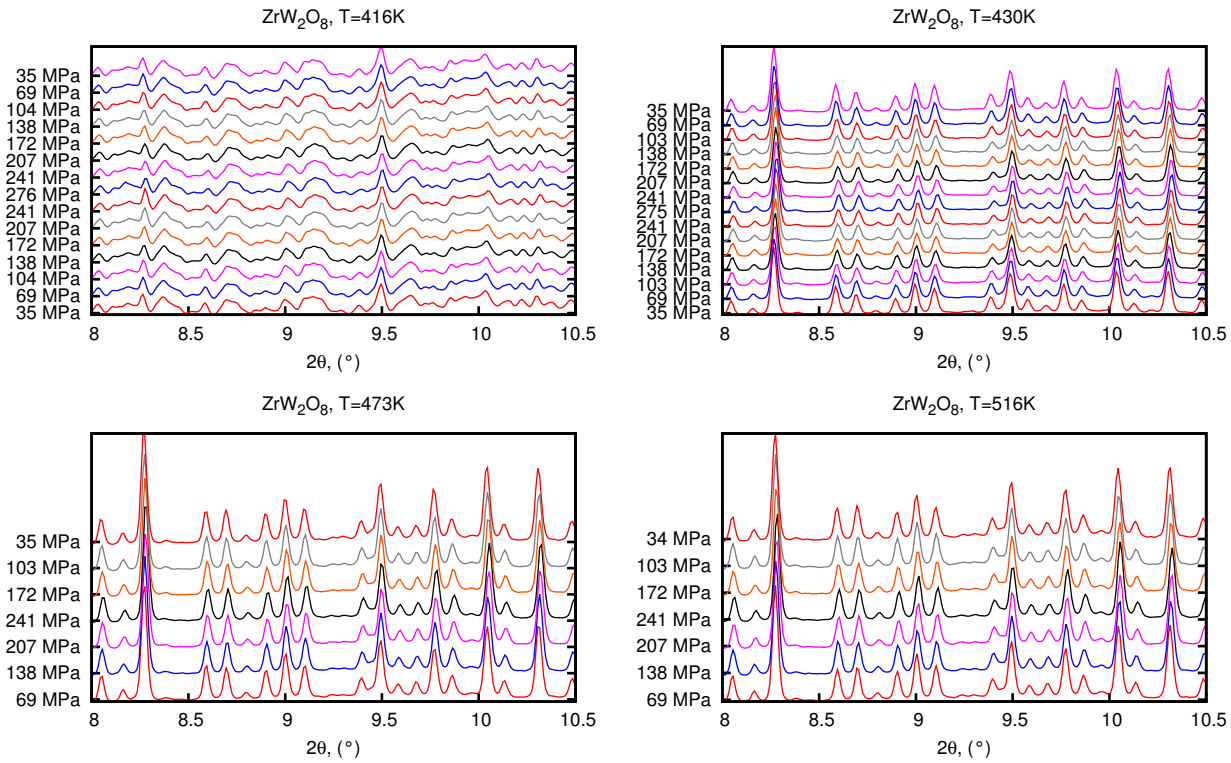

Sup. Fig. 6 Integrated diffraction data from ZrW_2O_8 experiment conducted in the MK2BRIM, 416-516K. Data are arranged in order of collection from bottom to top in each plot. Reversible pressure-dependent structural changes can be observed by inspection at 430K.

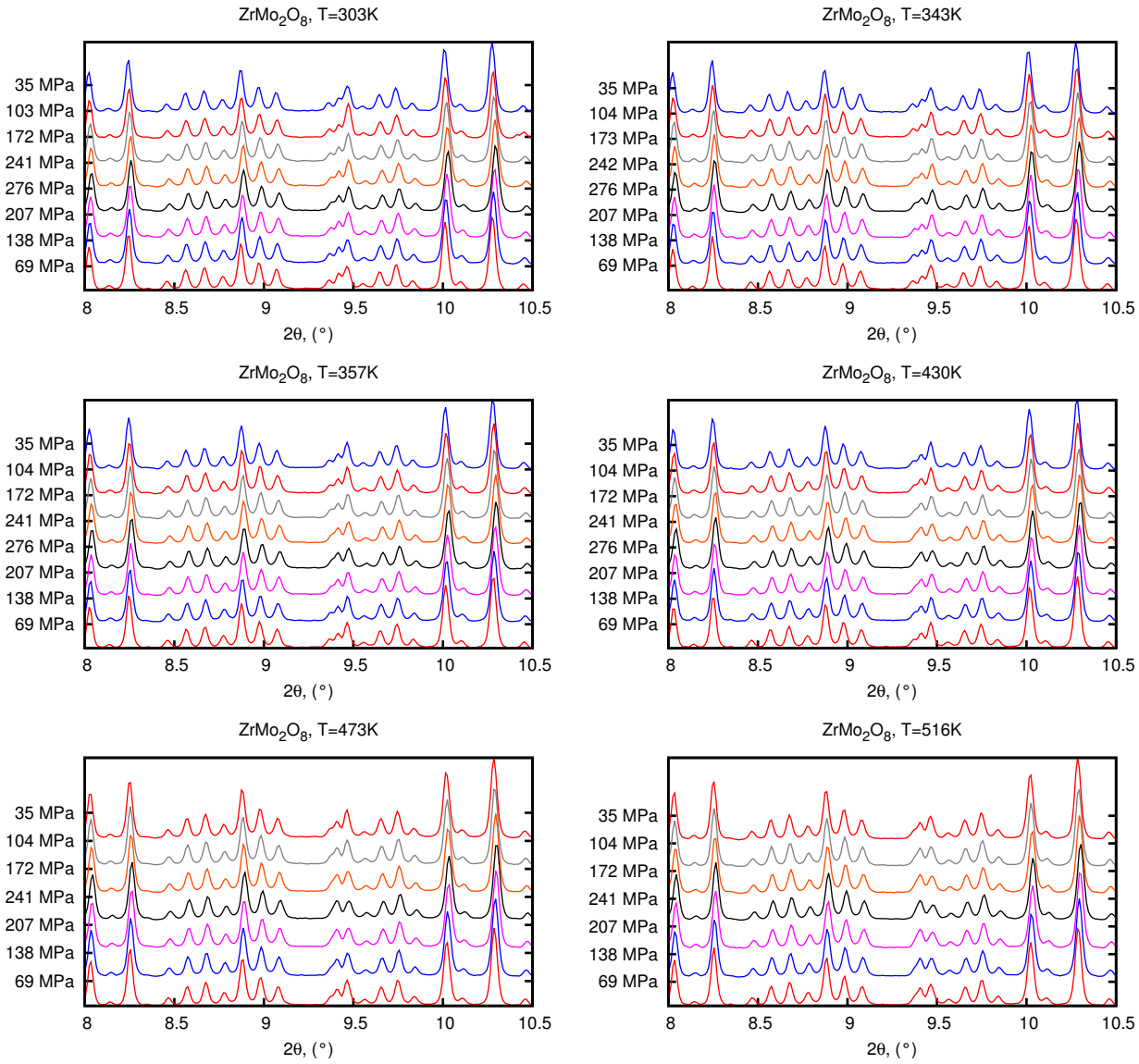

Sup. Fig. 7 Integrated diffraction data from $ZrMo_2O_8$ experiment conducted in the MK2BRIM. Data are arranged in order of collection from bottom to top in each plot. Absence of dramatic changes in structure upon heating or compression confirms the expected lack of a phase transition within the studied temperature and pressure ranges.

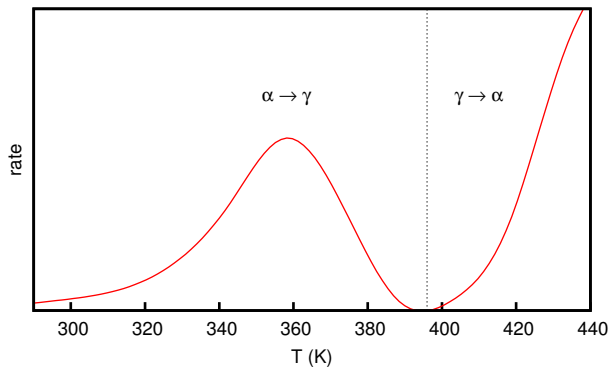

Sup. Fig. 8 Schematic showing the temperature dependence of the $\alpha \leftrightarrow \gamma$ transition rate for ZrW_2O_8 at 276 MPa between room temperature and 430K. Proposed trends are based on the non-equilibrium phase diagram generated from the MK2BRIM experiment (Figure 2) and the absence of any $\alpha \rightarrow \gamma$ transitions in the MK3BRIM experiment at 386K (Figure 3).

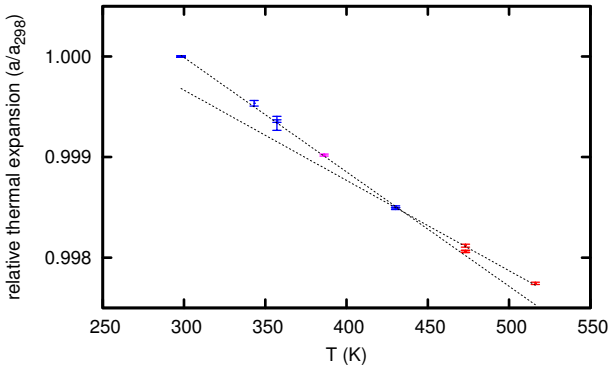

Sup. Fig. 9 Relative linear thermal expansion (a/a_{298K}) of ZrW_2O_8 at 35 MPa. The α phase is indicated by dark blue (MK2BRIM experiment) and pink (MK3BRIM experiment); the β phase is indicated by red symbols. The coefficent of thermal expansion calculated between room temperature and the $\alpha \rightarrow \beta$ transition temperature (423K) agrees well with that calculated from lattice constants published in previous literature[2] (-11 ppm·K^{-1} vs -13 ppm·K^{-1}), as does that calculated between 423K and 516K (-9 ppm·K^{-1} vs -8 ppm·K^{-1}).

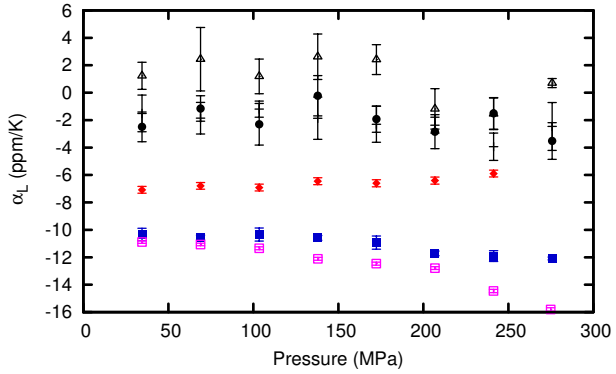

Sup. Fig. 10 Coefficients of thermal expansion of ZrW_2O_8. The α phase is denoted by either dark blue (MK2BRIM: 298K, 343K, and 357K) or pink (MK3BRIM: 298K and 386K) symbols; the γ phase (MK2BRIM: 357K, 371K, 386K, 401K, and 416K) is denoted by black symbols; the β phase (473K and 516K for ZrW_2O_8) is denoted by red symbols. Of note is that the CTEs obtained for the γ phase are nowhere near as negative as the CTEs of the cubic phases. The results for the γ phase are sufficiently noisy that no clear pressure dependence can be observed in the CTE.

Space group	T	κ^a (GPa)	κ^b(GPa)
$P2_13$	298K	64.2(10)	63.1(14)
$P2_13$	343K	59.9(9)	–
$P2_13$	357K	59.0(8)	–
$P2_12_12_1$	357K	60.2(15)	–
$P2_12_12_1$	371K	61.4(8)	–
$P2_12_12_1$	386K	60.0(8)	–
$P2_13$	386K	–	47.4(21)
$P2_12_12_1$	401K	59.0(7)	–
$P2_12_12_1$	416K	57.0(6)	–
$P2_13$	416K	41.4(5)	–
$P2_13$(high T)	430K	45.5(4)	–
$Pa\bar{3}$	473K	53.6(3)	54.0(11)
$Pa\bar{3}$	516K	55.5(2)	–

Sup. Table 2 Bulk moduli of ZrW_2O_8 obtained from MK2BRIM[a] and MK3BRIM[b] experiments.

Space group	T	κ (GPa)
$Pa3$	303K	43.3(5)
$Pa\bar{3}$	343K	43.3(4)
$Pa\bar{3}$	386K	44.4(4)
$Pa\bar{3}$	430K	45.1(4)
$Pa\bar{3}$	473K	45.3(2)
$Pa\bar{3}$	516K	45.0(2)

Sup. Table 3 Bulk moduli of $ZrMo_2O_8$ obtained from MK2BRIM experiment.

Sup. Table 4: Lattice constants obtained from ZrW_2O_8 MK2BRIM experiment, cubic models

Space group	T	P (MPa)	a (Å)	σ_a	Volume (Å^3)	σ_V
$P2_13$	298K	35	9.115350	0.000067	757.391	0.017
$P2_13$	298K	69	9.114000	0.000071	757.054	0.018
$P2_13$	298K	103	9.111990	0.000060	756.553	0.015
$P2_13$	298K	138	9.110690	0.000065	756.229	0.016
$P2_13$	298K	172	9.108770	0.000062	755.752	0.015
$P2_13$	298K	207	9.107460	0.000066	755.427	0.016
$P2_13$	298K	241	9.105700	0.000067	754.987	0.017
$P2_13$	298K	275	9.103940	0.000064	754.551	0.016
$P2_13$	343K	35	9.111110	0.000254	756.334	0.063
$P2_13$	343K	69	9.109670	0.000069	755.976	0.017
$P2_13$	343K	103	9.107750	0.000270	755.497	0.067
$P2_13$	343K	138	9.106350	0.000075	755.149	0.019
$P2_13$	343K	172	9.104290	0.000272	754.637	0.068
$P2_13$	343K	207	9.102660	0.000072	754.232	0.018
$P2_13$	343K	241	9.100820	0.000219	753.774	0.054
$P2_13$	343K	275	9.098990	0.000115	753.320	0.029
$P2_13$	357K	35	9.109500	0.000112	755.933	0.028
$P2_13$	357K	35	9.109290	0.000631	755.882	0.157
$P2_13$	357K	69	9.107800	0.000121	755.511	0.030
$P2_13$	357K	69	9.107770	0.000632	755.503	0.157
$P2_13$	357K	104	9.106050	0.000129	755.076	0.032
$P2_13$	357K	103	9.106320	0.000628	755.142	0.156
$P2_13$	357K	138	9.104470	0.000122	754.683	0.030
$P2_13$	357K	138	9.104490	0.000684	754.686	0.170
$P2_13$	357K	172	9.102710	0.000123	754.244	0.031
$P2_13$	357K	172	9.102460	0.000676	754.183	0.168
$P2_13$	357K	207	9.100860	0.000139	753.784	0.035
$P2_13$	357K	206	9.100980	0.000615	753.815	0.153
$P2_13$	357K	241	9.098830	0.000151	753.280	0.037
$P2_13$	357K	241	9.098840	0.000519	753.283	0.129
$P2_13$	357K	276	9.096910	0.000258	752.804	0.064
$P2_13$(high T)	298K	35	9.115340	0.000064	757.389	0.016
$P2_13$(high T)	298K	69	9.113980	0.000069	757.050	0.017
$P2_13$(high T)	298K	103	9.111970	0.000059	756.550	0.015
$P2_13$(high T)	298K	138	9.110680	0.000064	756.226	0.016
$P2_13$(high T)	298K	172	9.108760	0.000059	755.748	0.015
$P2_13$(high T)	298K	207	9.107450	0.000064	755.424	0.016
$P2_13$(high T)	298K	241	9.105680	0.000065	754.984	0.016
$P2_13$(high T)	298K	275	9.103940	0.000064	754.550	0.016
$P2_13$(high T)	430K	35	9.101570	0.000087	753.962	0.022
$P2_13$(high T)	430K	35	9.101730	0.000089	754.001	0.022
$P2_13$(high T)	430K	69	9.099320	0.000089	753.403	0.022
$P2_13$(high T)	430K	69	9.099220	0.000092	753.377	0.023
$P2_13$(high T)	430K	103	9.096880	0.000094	752.795	0.023
$P2_13$(high T)	430K	103	9.096810	0.000097	752.780	0.024
$P2_13$(high T)	430K	138	9.094380	0.000100	752.175	0.025
$P2_13$(high T)	430K	138	9.094360	0.000099	752.170	0.025
$P2_13$(high T)	430K	172	9.092090	0.000105	751.608	0.026
$P2_13$(high T)	430K	172	9.092130	0.000101	751.618	0.025

continued on next page

Sup. Table 4: Lattice constants obtained from ZrW_2O_8 MK2BRIM experiment, cubic models–continued from previous page

Space group	T	P (MPa)	a (Å)	σ_a	Volume (Å^3)	σ_V
$P2_13$(high T)	430K	207	9.090040	0.000104	751.100	0.026
$P2_13$(high T)	430K	207	9.090030	0.000102	751.096	0.025
$P2_13$(high T)	430K	241	9.087780	0.000103	750.539	0.026
$P2_13$(high T)	430K	241	9.087830	0.000105	750.551	0.026
$P2_13$(high T)	430K	275	9.085650	0.000104	750.012	0.026
$P2_13$(high T)	473K	35	9.097680	0.000093	752.995	0.023
$P2_13$(high T)	473K	69	9.095800	0.000092	752.527	0.023
$P2_13$(high T)	473K	103	9.093900	0.000093	752.057	0.023
$P2_13$(high T)	473K	138	9.091870	0.000098	751.553	0.024
$P2_13$(high T)	473K	172	9.090020	0.000094	751.095	0.023
$P2_13$(high T)	473K	207	9.088020	0.000097	750.599	0.024
$P2_13$(high T)	473K	241	9.085970	0.000096	750.091	0.024
$Pa\bar{3}$	473K	35	9.097690	0.000097	752.997	0.024
$Pa\bar{3}$	473K	69	9.095800	0.000098	752.527	0.024
$Pa\bar{3}$	473K	103	9.093910	0.000099	752.058	0.024
$Pa\bar{3}$	473K	138	9.091870	0.000104	751.554	0.026
$Pa\bar{3}$	473K	172	9.090020	0.000100	751.094	0.025
$Pa\bar{3}$	473K	207	9.088020	0.000102	750.598	0.025
$Pa\bar{3}$	473K	241	9.085970	0.000103	750.090	0.026
$Pa\bar{3}$	516K	34	9.094790	0.000106	752.278	0.026
$Pa\bar{3}$	516K	69	9.093020	0.000104	751.837	0.026
$Pa\bar{3}$	516K	103	9.091080	0.000106	751.358	0.026
$Pa\bar{3}$	516K	138	9.089230	0.000105	750.899	0.026
$Pa\bar{3}$	516K	172	9.087320	0.000109	750.426	0.027
$Pa\bar{3}$	516K	207	9.085400	0.000109	749.949	0.027
$Pa\bar{3}$	516K	241	9.083560	0.000103	749.493	0.026

Sup. Table 4 Lattice constants obtained from ZrW_2O_8 MK2BRIM experiment. Cubic models were fit to data based on visual inspection of XRD patterns.

Sup. Table 5: Lattice constants obtained from ZrW_2O_8 MK2BRIM experiment, $P2_12_12_1$ model

$P2_12_12_1$	P (MPa)	a (Å)	σ_a	b (Å)	σ_b	c (Å)	σ_c	Volume (Å^3)	σ_V
357K	35	9.033827	0.001105	26.928738	0.003072	8.880258	0.001125	2160.296	0.350
357K	35	9.033233	0.000671	26.919950	0.001850	8.880396	0.000681	2159.483	0.209
357K	69	9.029486	0.001172	26.923830	0.003265	8.878078	0.001197	2158.335	0.373
357K	69	9.031701	0.000656	26.914082	0.001811	8.879092	0.000666	2158.329	0.204
357K	104	9.029593	0.001146	26.916063	0.003183	8.875854	0.001170	2157.197	0.362
357K	103	9.029926	0.000662	26.909615	0.001821	8.876754	0.000672	2156.979	0.206
357K	138	9.027816	0.001043	26.911335	0.002898	8.876217	0.001065	2156.482	0.328
357K	138	9.027968	0.000690	26.905754	0.001897	8.875230	0.000700	2155.832	0.215
357K	172	9.025635	0.000995	26.905800	0.002755	8.873708	0.001014	2154.908	0.313
357K	172	9.026060	0.000673	26.899986	0.001847	8.873649	0.000682	2154.530	0.209
357K	207	9.024323	0.000969	26.899780	0.002666	8.870747	0.000984	2153.394	0.304
357K	206	9.024935	0.000679	26.895552	0.001859	8.872137	0.000688	2153.539	0.211
357K	241	9.022320	0.000862	26.892941	0.002367	8.870162	0.000877	2152.227	0.269
357K	241	9.022868	0.000705	26.891285	0.001935	8.871198	0.000716	2152.477	0.219
357K	276	9.021348	0.000735	26.886475	0.002013	8.868859	0.000746	2151.162	0.228
371K	35	9.035396	0.000864	26.913536	0.002399	8.880079	0.000877	2159.408	0.267
371K	35	9.034789	0.000807	26.913685	0.002230	8.879290	0.000820	2159.083	0.250

continued on next page

Sup. Table 5: Lattice constants obtained from ZrW_2O_8 MK2BRIM experiment, $P2_12_12_1$ model–continued from previous page

$P2_12_12_1$	P (MPa)	a (Å)	σ_a	b (Å)	σ_b	c (Å)	σ_c	Volume (Å^3)	σ_V
371K	69	9.033370	0.000848	26.907995	0.002353	8.878286	0.000862	2158.044	0.262
371K	69	9.032562	0.000798	26.909218	0.002197	8.877742	0.000812	2157.817	0.247
371K	103	9.031170	0.000852	26.904013	0.002355	8.876626	0.000867	2156.795	0.263
371K	103	9.030974	0.000809	26.903774	0.002226	8.876452	0.000825	2156.688	0.251
371K	138	9.029393	0.000829	26.898870	0.002281	8.874425	0.000844	2155.425	0.256
371K	138	9.029380	0.000807	26.896675	0.002225	8.874760	0.000821	2155.327	0.248
371K	172	9.027959	0.000840	26.893549	0.002315	8.873411	0.000855	2154.410	0.259
371K	172	9.027145	0.000811	26.892899	0.002228	8.873269	0.000825	2154.129	0.250
371K	207	9.025835	0.000848	26.888582	0.002330	8.871732	0.000861	2153.097	0.261
371K	207	9.025710	0.000784	26.890322	0.002147	8.871824	0.000796	2153.229	0.242
371K	241	9.024328	0.000839	26.885792	0.002298	8.869975	0.000851	2152.089	0.259
371K	241	9.024035	0.000806	26.884281	0.002203	8.869631	0.000819	2151.814	0.248
371K	275	9.022168	0.000782	26.880384	0.002134	8.868306	0.000792	2150.736	0.241
386K	35	9.034976	0.000822	26.914341	0.002273	8.879451	0.000835	2159.220	0.254
386K	35	9.034276	0.000789	26.912695	0.002185	8.879498	0.000803	2158.932	0.244
386K	69	9.032907	0.000819	26.910742	0.002258	8.877645	0.000832	2157.998	0.254
386K	69	9.032710	0.000795	26.906971	0.002200	8.877633	0.000810	2157.645	0.245
386K	103	9.031017	0.000789	26.902679	0.002168	8.875833	0.000804	2156.460	0.244
386K	103	9.030811	0.000851	26.903334	0.002342	8.875420	0.000866	2156.362	0.263
386K	138	9.029686	0.000789	26.898991	0.002163	8.873751	0.000802	2155.340	0.244
386K	138	9.028517	0.000800	26.898090	0.002197	8.874248	0.000814	2155.110	0.247
386K	172	9.027388	0.000783	26.895826	0.002146	8.872721	0.000795	2154.288	0.242
386K	172	9.027098	0.000780	26.893660	0.002133	8.872595	0.000794	2154.015	0.241
386K	206	9.025457	0.000785	26.890154	0.002154	8.870955	0.000796	2152.945	0.242
386K	207	9.025181	0.000809	26.889709	0.002216	8.870761	0.000821	2152.796	0.250
386K	241	9.023182	0.000748	26.885357	0.002041	8.869300	0.000760	2151.617	0.231
386K	241	9.023390	0.000776	26.884369	0.002115	8.869005	0.000787	2151.515	0.239
386K	275	9.021426	0.000751	26.880436	0.002041	8.867529	0.000761	2150.375	0.232
401K	35	9.034640	0.000775	26.915199	0.002137	8.878999	0.000787	2159.099	0.240
401K	35	9.034725	0.000777	26.914009	0.002142	8.879044	0.000789	2159.034	0.240
401K	69	9.032587	0.000761	26.912212	0.002099	8.877579	0.000773	2158.023	0.236
401K	69	9.032337	0.000743	26.908945	0.002047	8.877836	0.000756	2157.764	0.230
401K	103	9.030922	0.000763	26.905695	0.002105	8.876101	0.000774	2156.744	0.235
401K	103	9.030573	0.000781	26.904005	0.002148	8.875749	0.000795	2156.439	0.241
401K	138	9.028810	0.000777	26.901340	0.002123	8.874467	0.000791	2155.493	0.241
401K	138	9.028955	0.000788	26.898432	0.002166	8.874598	0.000802	2155.327	0.243
401K	172	9.027188	0.000758	26.895430	0.002077	8.872859	0.000769	2154.242	0.234
401K	172	9.026670	0.000783	26.894907	0.002145	8.872795	0.000796	2154.061	0.242
401K	207	9.025253	0.000765	26.889690	0.002083	8.870920	0.000777	2152.851	0.236
401K	207	9.025010	0.000809	26.887310	0.002208	8.871122	0.000822	2152.651	0.249
401K	241	9.023277	0.000750	26.884680	0.002042	8.869348	0.000760	2151.596	0.231
401K	241	9.022954	0.000767	26.882910	0.002089	8.869455	0.000777	2151.404	0.236
401K	276	9.021502	0.000744	26.880951	0.002020	8.867369	0.000754	2150.395	0.230
416K	35	9.037423	0.001540	26.908182	0.004323	8.878519	0.001550	2159.084	0.472
416K	35	9.037197	0.001538	26.906170	0.004316	8.878809	0.001550	2158.939	0.470
416K	69	9.034838	0.001545	26.904308	0.004322	8.876683	0.001558	2157.709	0.474
416K	69	9.034980	0.001508	26.901140	0.004227	8.877053	0.001522	2157.579	0.461
416K	103	9.032659	0.001512	26.898544	0.004227	8.874970	0.001525	2156.311	0.463
416K	104	9.032656	0.001493	26.895969	0.004178	8.875211	0.001509	2156.162	0.456

continued on next page

Sup. Table 5: Lattice constants obtained from ZrW_2O_8 MK2BRIM experiment, $P2_12_12_1$ model–continued from previous page

$P2_12_12_1$	P (MPa)	a (Å)	σ_a	b (Å)	σ_b	c (Å)	σ_c	Volume (Å^3)	σ_V
416K	138	9.030670	0.001417	26.894419	0.003956	8.873328	0.001429	2155.106	0.434
416K	138	9.030410	0.001472	26.891533	0.004112	8.873560	0.001488	2154.869	0.450
416K	172	9.028961	0.001429	26.891043	0.003972	8.871239	0.001441	2153.921	0.438
416K	172	9.028088	0.001410	26.887859	0.003927	8.871840	0.001425	2153.603	0.431
416K	207	9.026505	0.001406	26.884062	0.003898	8.869687	0.001417	2152.399	0.430
416K	207	9.026462	0.001379	26.884754	0.003826	8.869377	0.001391	2152.369	0.423
416K	241	9.024359	0.001404	26.881804	0.003873	8.867377	0.001413	2151.146	0.432
416K	241	9.024806	0.001384	26.880577	0.003822	8.867337	0.001393	2151.145	0.424
416K	276	9.022848	0.001367	26.874067	0.003772	8.866192	0.001374	2149.880	0.418

Sup. Table 5 Lattice constants obtained from ZrW_2O_8 MK2BRIM experiment. A $P2_12_12_1$ model was fit to the data for XRD patterns where it was evident by visual inspection that the $\alpha \rightarrow \gamma$ transition had occurred.

Sup. Table 6: Lattice constants obtained from ZrW_2O_8 MK3BRIM experiment, cubic models

Space group	T	P (MPa)	a (Å)	σ_a	Volume (Å^3)	σ_V
$P2_13$	298K	69	9.109929	0.000071	756.040	0.018
$P2_13$	298K	138	9.106708	0.000070	755.239	0.019
$P2_13$	298K	207	9.103127	0.000064	754.348	0.016
$P2_13$	298K	276	9.099586	0.000077	753.468	0.019
$P2_13$	298K	241	9.101390	0.000077	753.916	0.019
$P2_13$	298K	172	9.104658	0.000070	754.729	0.017
$P2_13$	298K	103	9.107805	0.000071	755.512	0.018
$P2_13$	298K	35	9.111081	0.000067	756.327	0.017
$P2_13$	386K	69	9.100857	0.000081	753.784	0.020
$P2_13$	386K	138	9.096786	0.000100	752.773	0.025
$P2_13$	386K	207	9.092655	0.000102	751.748	0.029
$P2_13$	386K	275	9.086649	0.000127	750.259	0.031
$P2_13$	386K	241	9.089556	0.000115	750.979	0.029
$P2_13$	386K	172	9.094449	0.000113	752.193	0.028
$P2_13$	386K	103	9.098512	0.000098	753.201	0.024
$P2_13$	386K	35	9.102155	0.000089	754.106	0.022
$Pa\bar{3}$	473K	69	9.091865	0.000092	751.552	0.023
$Pa\bar{3}$	473K	138	9.087873	0.000110	750.562	0.027
$Pa\bar{3}$	473K	207	9.084460	0.000130	749.717	0.032
$Pa\bar{3}$	473K	241	9.082028	0.000116	749.115	0.029
$Pa\bar{3}$	473K	172	9.086291	0.000122	750.170	0.030
$Pa\bar{3}$	473K	103	9.089894	0.000101	751.063	0.025
$Pa\bar{3}$	473K	35	9.093941	0.000136	752.067	0.034
$P2_13$ (high T)	386K	69	9.100851	0.000073	753.782	0.018
$P2_13$ (high T)	386K	138	9.096766	0.000075	752.768	0.019
$P2_13$ (high T)	386K	207	9.092649	0.000089	751.746	0.022
$P2_13$ (high T)	386K	275	9.086608	0.000092	750.249	0.023
$P2_13$ (high T)	386K	241	9.089545	0.000090	750.977	0.022
$P2_13$ (high T)	386K	172	9.094435	0.000084	752.189	0.021
$P2_13$ (high T)	386K	103	9.098514	0.000084	753.202	0.021
$P2_13$ (high T)	386K	35	9.102149	0.000088	754.105	0.022

Sup. Table 6 Lattice constants obtained from ZrW_2O_8 MK3BRIM experiment. Cubic models were fit to data based on visual inspection of XRD patterns.

Sup. Table 7: Lattice constants obtained from $ZrMo_2O_8$ MK2BRIM experiment, $Pa\bar{3}$ model

$Pa\bar{3}$	P (MPa)	a (Å)	σ_a	Volume (Å^3)	σ_V
303K	1	9.129006	0.000117	760.800	0.029
303K	69	9.124648	0.000121	759.711	0.030
303K	138	9.119946	0.000128	758.537	0.032
303K	207	9.114957	0.000133	757.293	0.033
303K	35	9.126906	0.000140	760.275	0.035
303K	276	9.109618	0.000140	755.963	0.035
303K	241	9.112365	0.000143	756.647	0.036
303K	172	9.117344	0.000148	757.888	0.037
303K	103	9.122045	0.000160	759.061	0.040
343K	35	9.125693	0.000139	759.972	0.035
343K	69	9.123399	0.000133	759.399	0.033
343K	104	9.121072	0.000140	758.818	0.035
343K	138	9.118667	0.000135	758.218	0.034
343K	173	9.116313	0.000139	757.631	0.035
343K	207	9.113846	0.000137	757.016	0.034
343K	242	9.111281	0.000135	756.377	0.034
343K	276	9.108767	0.000138	755.751	0.034
386K	35	9.123287	0.000145	759.371	0.036
386K	69	9.121164	0.000139	758.841	0.035
386K	104	9.118836	0.000145	758.260	0.036
386K	138	9.116542	0.000144	757.688	0.036
386K	172	9.114147	0.000144	757.091	0.036
386K	207	9.111759	0.000146	756.496	0.036
386K	241	9.109289	0.000146	755.881	0.036
386K	276	9.106862	0.000149	755.277	0.037
430K	35	9.120367	0.000153	758.642	0.038
430K	69	9.118298	0.000150	758.126	0.037
430K	104	9.115992	0.000147	757.551	0.037
430K	138	9.113698	0.000147	756.979	0.037
430K	172	9.111425	0.000145	756.413	0.036
430K	207	9.108988	0.000150	755.806	0.037
430K	241	9.106637	0.000147	755.221	0.037
430K	276	9.104217	0.000150	754.619	0.037
473K	35	9.118218	0.000149	758.106	0.037
473K	69	9.116005	0.000151	757.554	0.038
473K	104	9.113730	0.000146	756.987	0.036
473K	138	9.111430	0.000147	756.414	0.037
473K	172	9.109104	0.000145	755.835	0.036
473K	207	9.106725	0.000151	755.243	0.038
473K	241	9.104398	0.000150	754.664	0.037
516K	35	9.116366	0.000146	757.644	0.036
516K	69	9.114191	0.000147	757.102	0.037
516K	104	9.111843	0.000148	756.517	0.037
516K	138	9.109546	0.000149	755.945	0.037
516K	172	9.107220	0.000152	755.366	0.038
516K	207	9.104828	0.000150	754.771	0.037
516K	241	9.102471	0.000150	754.185	0.037

Sup. Table 7 Lattice constants obtained from $ZrMo_2O_8$ experiment. Cubic models were fit to data based on visual inspection of XRD patterns.

References

1 A. P. Wilkinson, C. R. Morelock, B. K. Greve, A. C. Jupe, K. W. Chapman, P. J. Chupas and C. Kurtz, *J. Appl. Crystallogr.*, 2011, **44**, 1047–1053.
2 J. S. O. Evans, T. A. Mary, T. Vogt, M. A. Subramanian and A. W. Sleight, *Chem. Mater.*, 1996, **8**, 2809–2823.